Impurity screening in strongly coupled plasma systems

2003 J. Phys. A: Math. Gen. 36 6235

(http://iopscience.iop.org/0305-4470/36/22/353)

INSTITUTE OF PHYSICS PUBLISHING JOURNAL OF PHYSICS A: MATHEMATICAL AND GENERAL

J. Phys. A: Math. Gen. **36** (2003) 6235–6241 PII: S0305-4470(03)55339-2

Impurity screening in strongly coupled plasma systems

Stamatios Kyrkos and Gabor J Kalman

Department of Physics, Boston College, Chestnut Hill, MA 02467, USA

E-mail: kyrkos@bc.edu

Received 28 October 2002, in final form 20 January 2003
Published 22 May 2003
Online at stacks.iop.org/JPhysA/36/6235

Abstract
We present an overview of the problem of screening of an impurity in a strongly coupled one-component plasma within the framework of the linear response (LR) theory. We consider 3D, 2D and quasi-2D layered systems. For a strongly coupled plasma the LR can be determined by way of the known $S(k)$ structure functions. In general, an oscillating screening potential with local overscreening and antiscreening regions emerges. In the case of the bilayer, this phenomenon becomes global, as overscreening develops in the layer of the impurity and antiscreening in the adjacent layer. We comment on the limitations of the LR theory in the strong coupling situation.

PACS numbers: 52.27.Gr, 68.65.Ac

1. Introduction

A large variety of condensed matter systems can be described as strongly coupled Coulomb systems. Examples are quantum wells and quantum dots in semiconductors, liquid metals, electrolytes, interiors of giant planets, white dwarfs etc. In a somewhat different setting, they also occur in dusty plasmas and charged colloids. This paper reviews and extends the information on the linear screening of an impurity $\rho_{\text{ext}} = Ze\delta(r)$ in various strongly coupled classical plasma systems. The term 'linear screening' indicates that the screening is determined via linear response theory (LR). Even when the plasma is strongly coupled, the coupling between the impurity may be weak or strong, depending on the charge Z of the impurity. In the former case the linear response theory should be adequate. The latter case is largely unexplored: one may introduce an effective potential [1–3], or, more reliably, resort to studying, either analytically or by computer simulation, impurity-plasma correlation functions in the $\rho_{\text{ext}} \to 0$ limit.

An improvement over the linear response theory could be provided by quadratic screening theory, which, however, has been analysed for weak coupling only [4–6]. The systems we consider are the three-dimensional (3D) one-component plasma (OCP), the 2D OCP and the OCP bilayer. While the basic features of the screening in 3D and 2D plasmas have been well known for a long time, the details of the screening for strong coupling have not been displayed. The issue of bilayers is fairly new (for references see [7]) and even the weak coupling analysis was only recently done [8]. Both the weak coupling and strong coupling scenarios exhibit some unexpected physical features.

The screening will be described in terms of the induced polarization density $\rho_{\rm pol} \equiv \rho$ and the resulting total (screened) potential $\Phi_{\rm tot}$. A parameter used in all cases is the plasma coupling parameter, which corresponds to the ratio of Coulomb energy to kinetic energy. For a system consisting of classical charged particles, the classical coupling parameter is $\Gamma = {Z_0}^2 e^2/(ak_B T)$, where a is the Wigner–Seitz radius and Z_0 is the charge of the plasma particles. The screening is generated through the polarization charge density of the medium that we assume to consist of particles of positive unit charge. The interaction potential (note that 'potential' is used here to designate potential energy) between the plasma particles is $\varphi(\mathbf{r})$ or its Fourier transform $\varphi(\mathbf{k})$. We take an impurity charge of $Z = -1$ (within the linear theory the sign of the charge is actually irrelevant and all the results scale with $|Z|$).

2. 3D strongly coupled OCP

In the model of the classical 3D OCP, a single species of particles is immersed in a neutralizing background. Its Wigner–Seitz radius is $a = (4n\pi/3)^{-1/3}$ and the traditional coupling parameter γ is related to Γ as $\gamma^2 = 3\Gamma^3$. The interaction potential is $\varphi(\mathbf{k}) = 4\pi e^2/k^2$. Then

$$\rho(\mathbf{k}) = \chi(\mathbf{k})\varphi(\mathbf{k})\rho_{\rm ext}(\mathbf{k}) = -\chi(\mathbf{k})\varphi(\mathbf{k}). \tag{1}$$

The full (screened) density response function $\chi(\mathbf{k})$ can be linked to the structure function $S(\mathbf{k})$ that has been available both through HNC calculations [9] and through Monte Carlo simulations [10] via the classical fluctuation–dissipation theorem (FDT)

$$S(\mathbf{k}) = -\frac{1}{\beta n}\chi(\mathbf{k}) \tag{2}$$

whence the polarization density becomes

$$\rho(\mathbf{k}) = S(\mathbf{k})\frac{\kappa_{\rm 3D}^2}{k^2} \tag{3}$$

($\kappa_{\rm 3D}^2 = 4\pi e^2 n$ is the 3D Debye wave number). The polarization potential $\Phi_{\rm pol}(\mathbf{k})$ and the total (screened) potential $\Phi_{\rm tot}(\mathbf{k})$ are

$$\Phi_{\rm pol}(\mathbf{k}) = \varphi(\mathbf{k})\rho(\mathbf{k}) = \varphi(\mathbf{k})\frac{\kappa_{\rm 3D}^2}{k^2}S(\mathbf{k}) \tag{4}$$

$$\begin{aligned}\Phi_{\rm tot}(\mathbf{k}) &= \Phi_{\rm pol}(\mathbf{k}) + \Phi_{\rm ext}(\mathbf{k})\\ &= -\varphi(\mathbf{k})\,[1-\rho(\mathbf{k})] = -\varphi(\mathbf{k})\,[1-\beta n\varphi(\mathbf{k})S(\mathbf{k})]\end{aligned} \tag{5}$$

where $\Phi_{\rm ext}(\mathbf{k})$ is the external potential due solely to the impurity.

The behaviour of $\Phi_{\rm tot}(r)$ is nonmonotonic, with local screening and antiscreening regions. Thus, a positive impurity would cause the total potential $\Phi_{\rm tot}(r)$ to become locally negative (see figures 1 and 2); such negative regions would correspond to strong attractive interaction between like particles. Asymptotically, for $r \to \infty$, the total potential is well known to drop off as $\mathrm{e}^{-\kappa r}/r$. At $r = 0$ the polarization potential assumes a finite value

$$\Phi_{\rm pol}(r=0) = -\frac{e^2}{a}\frac{2}{\pi}\int \mathrm{d}\bar{k}\,\frac{\kappa_{\rm 3D}^2}{\bar{k}^2}S(k) \tag{6}$$

which, in contrast to the Debye result, is, in general, different from twice the correlation energy per particle. (Here and in the following the notation $\bar{k} = ka$ is used.)

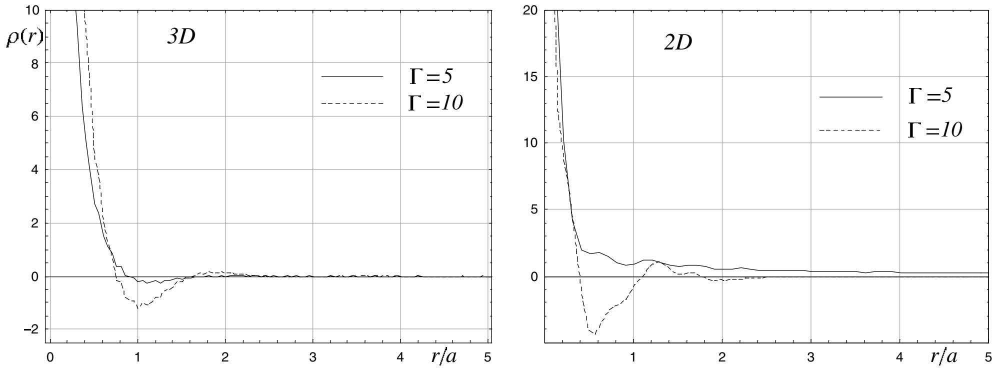

Figure 1. Polarization density $\rho(r)$, in units of equilibrium density n, for 2D and 3D systems for various Γ values.

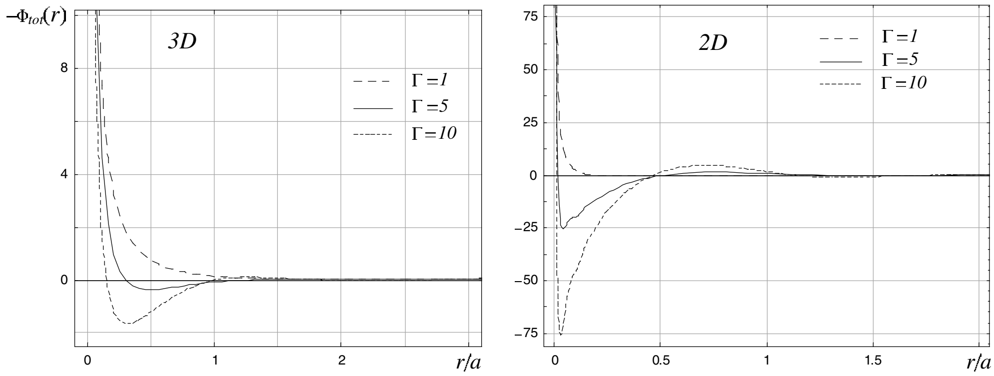

Figure 2. 3D and 2D $\Phi_{\mathrm{tot}}(r)$, in units of e^2/a. The potentials oscillate with alternating sign, indicating the overscreening and antiscreening regions.

3. 2D strongly coupled OCP

Proceeding the same way as in the preceding section, we now examine a classical 2D OCP. The Wigner–Seitz radius is $a = 1/\sqrt{\pi n}$ and the traditional plasma parameter γ is related to Γ as $\gamma = 2\Gamma^2$. The 2D interaction potential is $\varphi(\mathbf{k}) = 2\pi e^2/k$. Similarly to the 3D case, the structure function $S(\mathbf{k})$ is available both through HNC calculations [11] and through computer simulations [11, 12]. The polarization density now is

$$\rho(\mathbf{k}) = S(\mathbf{k})\frac{\kappa_{2\mathrm{D}}}{k} \tag{7}$$

($\kappa_{2\mathrm{D}} = 2\pi e^2 n/(k_B T)$ is the 2D Debye wave number). With the appropriate change in $\varphi(\mathbf{k})$, the expressions for the polarization potential $\Phi_{\mathrm{pol}}(r)$ and the total (screened) potential $\Phi_{\mathrm{tot}}(r)$ are similar to those in the 3D case.

As in the 3D OCP, $\Phi_{\mathrm{tot}}(r)$ exhibits a strong oscillatory behaviour (see figures 1 and 2). Remarkably, however, as shown in figure 3(a), the oscillation amplitudes for comparable Γ values are considerably higher in 2D than in 3D. Asymptotically, for $r \to \infty$, the total potential drops off as $1/r^3$, since the polarization charge and the impurity charge form a quadrupole-like distribution of charge. At $r = 0$ the polarization potential is now given by the

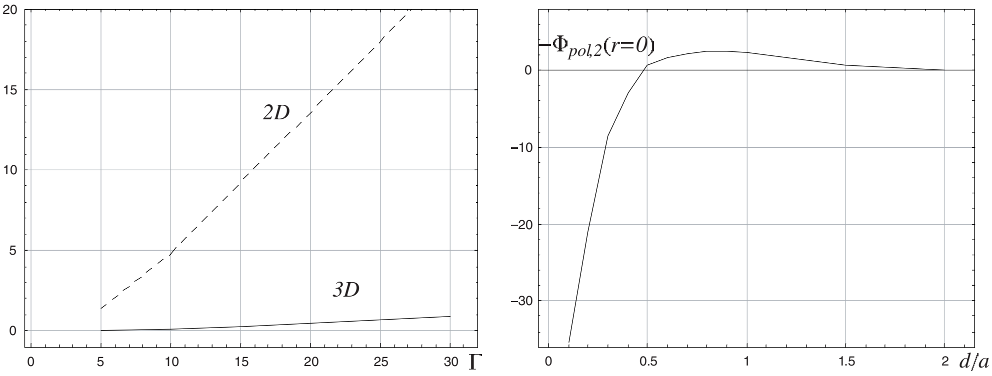

(*a*) (*b*)

Figure 3. (*a*) Comparison of the amplitudes of the first peak of $\Phi_{\mathrm{tot}}(r)$ for 2D and 3D. The oscillations in 2D are much more pronounced. (*b*) Second layer polarization potential $\Phi_{\mathrm{pol},2}$ at $r = 0$, as a function of interlayer distance d for $\Gamma = 20$ (units are the same as in figures 1 and 2).

unphysical logarithmically divergent integral

$$\Phi_{\mathrm{pol}}(r = 0) = -\frac{e^2}{a} \int \mathrm{d}\bar{k} \frac{\kappa_{2\mathrm{D}}}{\bar{k}} S(k) . \tag{8}$$

The correlation energy is, of course, finite.

4. Strongly coupled classical bilayers

The bilayer model we consider consists of two 2D layers of positively charged particles, separated by a distance d, of equal areal densities n and immersed in an oppositely charged neutralizing background. The impurity of charge $Z = -1$ is placed on layer 1. While in the weak coupling regime, $\Gamma < 1$, the random-phase approximation (RPA) is adequate in describing such systems (for a complete weak coupling description see [8]), at higher Γ values the RPA is no longer satisfactory. The results presented here rely on recent classical HNC generated structure functions [13, 14], corroborated by molecular dynamics simulations [15]. The interaction potential matrix is

$$\varphi(\mathbf{k}) = \begin{bmatrix} \varphi_{11} & \varphi_{12} \\ \varphi_{21} & \varphi_{22} \end{bmatrix} = \varphi(\mathbf{k}) \begin{bmatrix} 1 & \mathrm{e}^{-kd} \\ \mathrm{e}^{-kd} & 1 \end{bmatrix} \tag{9}$$

$\varphi(\mathbf{k}) = \frac{2\pi e^2}{k}$. The polarization densities ensue now from the matrix relation

$$\rho_i(\mathbf{k}) = -\chi_{ij}(\mathbf{k})\varphi_{j1}(\mathbf{k}). \tag{10}$$

The corresponding classical fluctuation dissipation theorem leads to

$$\begin{aligned} \rho_1(\mathbf{k}) &= \frac{\kappa_{2\mathrm{D}}}{k}[S_{11}(\mathbf{k}) + \mathrm{e}^{-kd} S_{12}(\mathbf{k})] \\ \rho_2(\mathbf{k}) &= \frac{\kappa_{2\mathrm{D}}}{k}[\mathrm{e}^{-kd} S_{11}(\mathbf{k}) + S_{12}(\mathbf{k})] \end{aligned} \tag{11}$$

with S_{11} and S_{12} the intralayer and interlayer structure functions, respectively. They obey the Stillinger–Lovett condition, such that $S_{11}(k = 0) + S_{12}(k = 0) = 0$. The total charges on each layer are $\rho_1(k = 0) - 1$ and $\rho_2(k = 0)$, respectively. Thence, the perfect screening sum rule requires that

$$\rho_1(k = 0) + \rho_2(k = 0) = +1. \tag{12}$$

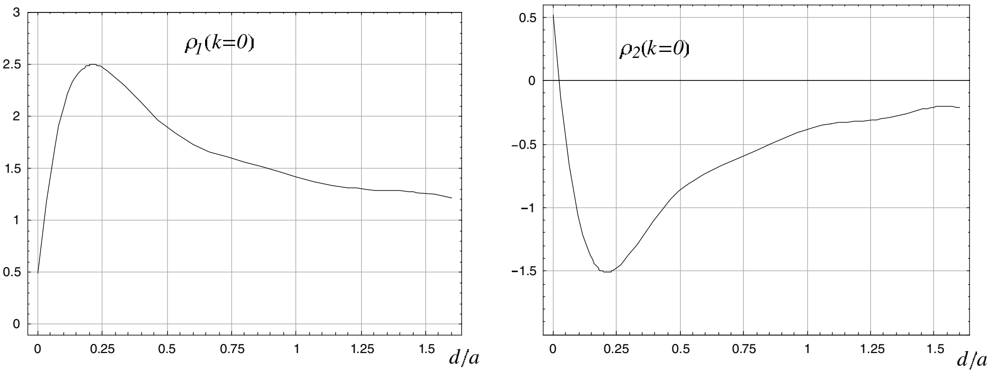

Figure 4. $\rho_1(k = 0)$ and $\rho_2(k = 0)$ as a function of d for $\Gamma = 20$. Note that ρ_2 changes sign for very small d.

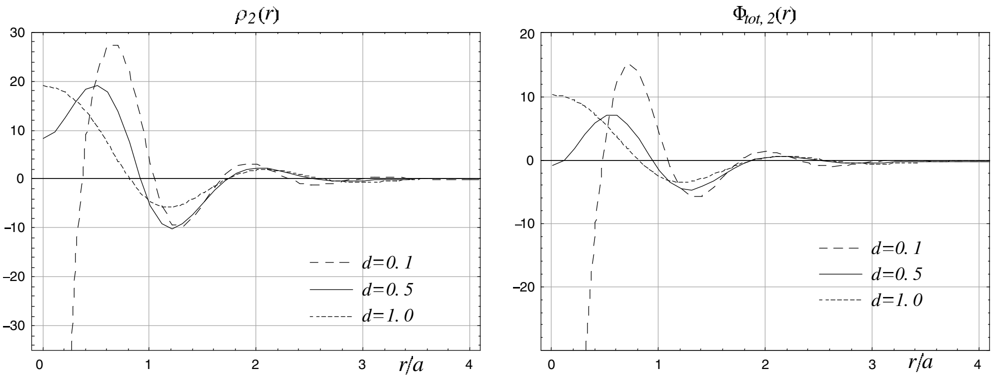

Figure 5. Polarization density $\rho(r)$, in units of equilibrium density n, and total (screened) potential $\Phi_{\mathrm{tot}}(r)$, in units of e^2/a, for layer 2 of a bilayer for $\Gamma = 20$.

The remarkable feature of the bilayer system is that in the strong coupling situation, while the requirement (12) is observed, each layer develops excess charges; layer 1 overscreens and, to compensate, layer 2 antiscreens the impurity charge [14]. The amount of the total polarization charges in the respective layers is dictated by the generalized compressibility sum rule [7]:

$$\begin{aligned} \rho_1(k=0) &= -\frac{1}{2}\frac{L-N+4\Gamma\bar{d}}{L-N+2\Gamma\bar{d}} \\ \rho_2(k=0) &= \frac{1}{2}\frac{L-N}{L-N+2\Gamma\bar{d}} \end{aligned} \tag{13}$$

where $\bar{d} = d/a$, and $L_{ij} = \frac{[\partial P_i/\partial n_j]_T}{[\partial P_0/\partial n]_T}$, and $L = L_{11} = L_{22}$, $N = L_{12} = L_{21}$ are the direct- and trans-inverse compressibility coefficients. For weak coupling both ρ_1 and ρ_2 are positive; in contrast, for strong coupling ρ_2 changes sign, and both ρ_1 and ρ_2 reach a sharp maximum (minimum) at a small $\bar{d}$ value (figure 4). The detailed charge distributions in the second layer is portrayed in figure 5. The corresponding total (screened) potential is given by

$$\begin{aligned} \Phi_{\mathrm{tot},1}(\mathbf{k}) &= -\varphi(\mathbf{k})\left\{1 + \frac{\kappa_{2\mathrm{D}}}{k}[(\mathrm{e}^{-kd}+1)S_{11}(\mathbf{k}) + 2\,\mathrm{e}^{-kd}S_{12}(\mathbf{k})]\right\} \\ \Phi_{\mathrm{tot},2}(\mathbf{k}) &= -\varphi(\mathbf{k})\left\{\mathrm{e}^{-kd} + \frac{\kappa_{2\mathrm{D}}}{k}[2\,\mathrm{e}^{-kd}S_{11}(\mathbf{k}) + (\mathrm{e}^{-kd}+1)S_{12}(\mathbf{k})]\right\} \end{aligned} \tag{14}$$

and is portrayed in figure 5. At $r = 0$, the behaviour of the polarization potential in layer 1 is similar to that of a 2D system, with the unphysical logarithmically divergent value. In layer 2, the polarization potential at $r = 0$ is finite and changes sign from positive to negative at a small $\bar{d}$ value, as shown in figure 3(*b*). An interesting and counterintuitive feature of the polarization potential at an arbitrary $r \neq 0$ is that it is a nonmonotonic function of the layer separation d. This has been demonstrated only for weak coupling [8], but it is expected to be the general feature inherent to layered systems.

5. Conclusions

The limitations of the linear response theory in the strong coupling situation are not well understood. However, from the results presented in this paper, it is probably safe to conclude that when the impurity charge is of the order of the charge of the plasma particles, the LR results are mostly unphysical. One easily available test is provided by assuming that the impurity is one of the plasma particles and then to compare the polarization density calculated from LR with the correlation density $\bar{\rho}$ around the 'impurity', as given by the equilibrium pair correlation function $\bar{\boldsymbol{\rho}}(\mathbf{k}) = (\mathbf{S} - \mathbf{I}) \cdot \boldsymbol{\rho}_{\mathrm{ext}}(\mathbf{k})$. The corresponding LR expression is $\boldsymbol{\rho}(\mathbf{k}) = \boldsymbol{\chi}(\mathbf{k}) \cdot \boldsymbol{\varphi}(\mathbf{k}) \cdot \boldsymbol{\rho}_{\mathrm{ext}}(\mathbf{k})$ and we see that strict equality $\bar{\rho} = \rho$ requires that χ satisfy the relation

$$\boldsymbol{\chi}(\mathbf{k}) = -\frac{\beta n \mathbf{I}}{\mathbf{I} + \beta \mathrm{n} \boldsymbol{\varphi}(\mathbf{k})} \tag{15}$$

($\mathbf{I}$ is the unit matrix). This is tantamount to the Debye description of weak coupling. Even though ρ and $\bar{\rho}$ are conceptually not quite identical (in one case the 'impurity' is thermally excited, in the other it is held at rest), the result can be taken as an indication that the linear response theory does not adequately describe scenarios where the coupling between the impurity and the plasma is of strength comparable to the coupling within the plasma. The situation can be quite different when the impurity charge Z is much smaller than the charge of the plasma particles Z_0. In this case, the LR theory is expected to provide a reasonable rendition of the novel physical effects brought about by the strong coupling, such as the strong oscillatory behaviour of the screened potential and the global overscreening/antiscreening behaviour in bilayer systems. A low Z/Z_0, high Γ situation may be realized in highly charged colloidal or complex (dusty) plasma systems. Preliminary results of molecular dynamics (MD) simulations [16] seem to corroborate the predictions of the LR theory for such systems.

Acknowledgments

This work has been partly supported by grants DE-FG02-98ER54501 and NSF PHYS0206695.

References

[1] Szymański J, Świerkowski L and Neilson D 1994 *Phys. Rev.* B **50** 11002
[2] Thakur J S, Neilson D and Das M P 1998 *Phys. Rev.* B **57** 1801
[3] Vignale G and Singwi K S 1985 *Phys. Rev.* B **31** 2729
[4] Percival D J and Robinson P A 1998 *Phys. Plasmas* **5** 1279
[5] Cenni R and Saracco P 1988 *Nucl. Phys.* A **487** 279
[6] Rommel J M, Kalman G J and Genga G 1998 *Strongly Coupled Coulomb Systems* ed G J Kalman, M J Rommel and K Blagoev (New York: Plenum) pp 669–72
Kalman G J and Golden K I 1993 *Condensed Matter Theories* vol 8 ed L Blum and F B Malik (New York: Plenum) pp 127–37
Tao Z C 1990 *PhD Thesis* Boston College

[7] Golden K I and Kalman G J 2003 *J. Phys. A: Math. Gen.* **36** 5865–75
[8] Golden K I, Kalman G K and Kyrkos Stamatios 2002 *Phys. Rev.* E **66** 031107
[9] Rogers F J, Young D A, DeWitt H E and Ross M 1983 *Phys. Rev.* A **28** 2990
[10] Slattery W L, Doolen G D and DeWitt H E 1980 *Phys. Rev.* A **21** 2087
[11] Gann R C, Chakravatry S and Chester G V 1979 *Phys. Rev.* B **20** 326
[12] Totsuji H and Kakeya H 1980 *Phys. Rev.* A **22** 1220
[13] Valtchinov V I, Kalman G J and Blagoev K B *Phys. Rev.* E **56** 4351
[14] Kalman G J, Donkó Z, Golden K I and McMullan G 2001 *Condensed Matter Theories 16* (New York: Nova Science Publishers) pp 51–9
Kalman G J *et al* 2000 *J. Phys.* IV **10** Pr5–117
[15] Donkó Z and Kalman G J 2001 *Phys. Rev.* E **63** 061504
[16] Donkó Z 2002 Private communication